Chemical Analysis of Impurity Boron Atoms in Diamond using Soft X-Ray Emission Spectroscopy

Yasuji MURAMATSU*, Junji IIHARA**, Toshihiko TAKEBE**, and Jonathan D. DENLINGER***

** Graduate School of Engineering, University of Hyogo, 2167 Shosha, Himeji, Hyogo 671-2201, Japan*

*** Sumitomo Electric Industries, Ltd., 1-1-1 Koya-kita, Itami, Hyogo 665-0016, Japan*

****Advanced Light Source, Lawrence Berkeley National Laboratory, 1Cyclotron Road, Berkeley, CA 94720, USA*

Abstract

To analyze the local structure and/or chemical states of boron atoms in boron-doped diamond, which can be synthesized by the microwave plasma-assisted chemical vapor deposition method (CVD-B-diamond) and the temperature gradient method at high pressure and high temperature (HPT-B-diamond), we measured the soft X-ray emission spectra in the C*K* and B*K* regions of B-diamonds using synchrotron radiation at the Advanced Light Source (ALS). X-ray spectral analyses using the fingerprint method and molecular orbital calculations confirm that boron atoms in CVD-B-diamond substitute for carbon atoms in the diamond lattice to form covalent B-C bonds, while boron atoms in HPT-B-diamond react with the impurity nitrogen atoms to form hexagonal boron nitride. This suggests that the high purity diamond without nitrogen impurities is necessary to synthesize *p*-type B-diamond semiconductors.

Introduction

Impurity-doped diamonds can be wide-gap semiconductors, which can be utilized as electron emitters and high-power amplifiers in electronic devices.[1] In particular, boron-doped diamond (denoted as B-diamond) has recently attracted much attention from technological application and materials science points of view. High-quality B-diamond has been synthesized by a microwave plasma-assisted chemical vapor deposition (CVD) method where the boron concentration controls its electrical properties.[2,3] To clarify the relationship between the electronic structure and local structure of the boron atoms in B-diamond, the valence band and conduction band have been analyzed by soft X-ray emission spectroscopy (XES) and absorption spectroscopy (XAS) using synchrotron radiation (SR).[4-6] These spectroscopic studies have elucidated that covalent B-C bond formation in a diamond matrix is important for acceptor formation in *p*-type B-diamond semiconductors. Additionally, superconducting characteristics have been discovered in heavily boron-doped diamond,[7] and its electronic structure has been analyzed by SR photoemission spectroscopy[8] and the X-ray scattering method.[9] These analytical studies on B-diamond using SR have suggested that the electronic structure strongly depends on the local structure and/or chemical states of the dopant boron atoms in the diamond lattice. On the other hand, chemical analyses of boron compounds using XES including the conventional X-ray fluorescence spectrometry have been achieved by many reseacheres.[10-19] This shows that XES is a powerful tool to investigate the chemical states of boron compounds.

As previously mentioned, the electronic structure of the high-quality B-diamond synthesized by the CVD method can be successfully analyzed by XES and XAS. However, B-diamond synthesized by a temperature gradient method at high pressure and high temperature (denoted by HPT)[20,21] has not been analyzed by XES and XAS yet. The difference between the CVD and HPT methods is the impurity nitrogen in the diamond matrix; CVD-diamond has a negligible nitrogen impurity, while HPT-diamond generally has ppm- or sub-ppm-orders of nitrogen as an impurity.[22] Therefore, it should be interesting to investigate the effects of impurity nitrogen on the local structure and/or chemical states of dopant boron.

In the present study, we analyzed dopant boron in the B-diamond synthesized by the HPT method using XES and compared it to CVD-B-diamond. Moreover, the local structure and/or

chemical states of dopant boron atoms in the B-diamonds are discussed using the spectral analysis of XES spectra and molecular orbital calculations.

Experiments

Two types of B-diamond samples were prepared. One was a boron-doped diamond-single-crystal film synthesized by the CVD method with methane, hydrogen, and diborane gases on single-crystal diamond substrates (denoted as CVD-B-diamond). The concentration of boron in CVD-B-diamond was evaluated by SIMS as 920 ppm. The other B-diamond sample was synthesized by the HPT method with a high-purity carbon source and boron source for the dopant (denoted as HPT-B-diamond). The concentration of boron in the HPT-B-diamond sample was adjusted to 300 ppm. Although the concentration of impurity nitrogen in the measured HPT-B-diamond sample was not unfortunately analyzed by SIMS, it can be estimated to be not less than several tens ppm. The High-purity CVD- and HPT-diamonds without boron doping were also synthesized as references. In addition, commercially available highly oriented pyrolytic graphite (HOPG), hexagonal boron nitride (*h*-BN), cubic boron nitride (*c*-BN), boron carbide (B_4C), and amorphous boron (*a*-B) were prepared as reference compounds.

Spectroscopic measurements of the soft X-ray emission in the B*K* and C*K* regions were performed with a grating X-ray spectrometer installed at beamline BL-8.0.1[23] of the Advanced Light Source (ALS). The emission spectra were obtained with excitation energies tuned to 230 eV for the B*K* region and 320 eV for the C*K* region in order to effectively excite the 1s-electrons and prevent multiple ionizations. The estimated resolving power (E/ΔE) of the spectrometer was 1300 for the B*K* measurements using a 40-μm entrance slit and a 1500-lines/mm spherical grating with a 5-m radius, and 680 for the C*K* measurements using a 600-lines/mm grating with a 10-m radius.

Results and Discussion

Figure 1 shows the C*K* X-ray emission spectra of the B-diamonds and reference compounds. All the diamond samples exhibited similar spectral profiles; a plateau in the region of 278 – 281 eV, a low-energy satellite at 272 eV, and a high-energy peak edge at 284 eV. This spectral profile

corresponds to previously published data.[24,25] Therefore, it is confirmed that CVD-B-diamond and HPT-B-diamond essentially take a typical diamond crystal structure. Figure 2 shows the B*K* X-ray emission spectra of CVD-B- and HPT-B-diamonds and reference boron compounds. The CVD-B-diamond exhibited a main peak around 184 eV with a steep edge at 185 eV and lower-energy tailing, which apparently differs from the spectral profiles of HTP-B-diamond, *h*-BN, and *c*-BN. Although B_4C and *a*-B exhibited similar spectral profiles with a main peak and lower-energy tailing of CVD-B-diamond, neither exhibited the steep 185-eV edge. This demonstrates that the chemical states of the dopant B atoms in the CVD-B-diamond differ from those of HTP-B-diamond and the reference compounds. The HPT-B-diamond exhibited a main peak at 182 eV, a high-energy shoulder at 185 eV, a low-energy shoulder at 178 eV, and a lower-energy satellite at 170 eV. This spectral profile corresponds to that of *h*-BN. Although *c*-BN also exhibited a similar profile, the main peak is broader than that of HPT-B-diamond and *h*-BN. This indicates that dopant B atoms in the HPT-B-diamond mainly form *h*-BN in the diamond matrix and the concentration of impurity N atoms in the HPT-B-diamond will be not less than 300 ppm.

To theoretically clarify the measured B*K* X-ray spectral profiles of the B-diamonds, we calculated the density of state (DOS) of the boron atoms with appropriate cluster models using the discrete variational (DV) –Xα method.[26,27] The calculated DOS was compared to the measured B*K* X-ray emission spectra. The upper panel of Fig. 3 shows the hydrogen-terminated cluster model, $BC_{146}(H_{148})$, for CVD-B-diamond where one B atom is substituted for the C atom bonded to the centered C atom in the diamond $C_{147}H_{148}$ cluster. The lower panel shows the occupied 2*p*- and 2*s*-DOS of the B atom and the centered C atom (denoted by asterisks in the figure) as well as compares them to the measured B*K* X-ray emission spectra of CVD-B-diamond. The B2*p*-DOS well reproduced the measured spectral profile. The B2*p*-DOS consisted of a main peak at -3 eV in the MO energy, a higher-energy shoulder at -1 eV, and lower-energy tailing. The high-energy shoulder in the B2*p*-DOS corresponds to the steep edge at 185 eV in the measured spectrum. The B2*p* orbitals at the higher-energy shoulder hybridize with the highest C2*p* orbitals, and the hybridized DOS can form the acceptor level in both the B and C atoms.[6] The lower-energy tailing in the B2*p*-DOS is mainly formed by the hybridization of B2*p* with B2*s* orbitals. Thus, the B*K* X-ray emission spectral profile of

CVD-B-diamond can be understood from the DOS of the B atoms in the diamond lattice. Hence, it is confirmed that the dopant B atoms in the CVD-B-diamond can substitute for carbon atoms in the diamond lattice to form covalent B-C bonds.

The upper panel of Fig. 4 shows the hydrogen-terminated cluster model, $B_{48}N_{48}(H_{24})$, for *h*-BN,[28] which was observed in the HPT-B-diamond. The lower panel shows the calculated occupied 2*p*- and 2*s*-DOS of the centered B and N atoms (denoted by asterisks in the figure) as well as compares them to the measured B*K* X-ray spectra of HPT-B-diamond and *h*-BN. The B2p-DOS well reproduced the measured spectral profile. The B2p-DOS consisted of a main peak at -5 eV, a higher-energy shoulder around -3 eV, a lower-energy shoulder around -9 eV, and a lower-energy satellite around -16 eV. The main peak and the higher-energy shoulder are mainly formed by the hybridization of B2*p* with the N2*p* orbitals. The lower-energy shoulder can be formed by the hybridization of B2*p* with B2*s* and N2*p*, while the lower-energy satellites are mainly formed by the hybridization of B2*p* with N2*s*. This satellite is a characteristic of the sp^2-coordinated B atoms in *h*-BN. Therefore, the B*K* X-ray emission spectral profile of HPT-B-diamond can be understood from the DOS in *h*-BN. Hence, it is confirmed that the dopant B atoms in the HPT-B-diamond can react with impurity N atoms in the diamond lattice to form *h*-BN clusters.

Conclusion

To analyze the local structures and/or chemical states of boron atoms in B-diamonds, which can be synthesized by the CVD method and the HPT method, the soft X-ray emission spectra in the B*K* and C*K* regions of the CVD-B-diamond and HPT-B-diamond were measured using synchrotron radiation at the ALS. Although the C*K* X-ray profiles of the CVD-B- and HPT-B-diamonds exhibited typical diamond profiles, CVD-B and HPT-B diamonds had different B*K* X-ray profiles. Spectral analysis using a fingerprint method suggested that the boron atoms in the HPT-B-diamond reacted with the impurity nitrogen atoms to form boron nitride in HPT-diamond. To clarify the local structure and/or chemical states of the boron atoms in the B-diamonds, the B*K* X-ray emission profiles of the CVD-B- and HPT-B-diamonds were compared to the B2*p*-DOS of the appropriate cluster models. The B*K* X-ray emission profile of CVD-B-diamond successfully explained the boron atoms substituting for

the carbon atoms in the diamond lattice, while *h*-BN profile explained the profile of HPT-B-diamond. Thus, it is elucidated that impurity nitrogen in the diamond interferes with the formation of covalent B-C bond formation in the diamond lattice, and that the CVD method is preferable for doping boron atoms into diamond in order to develop *p*-type B-diamond semiconductors.

Acknowledgments

The authors would like to express their gratitude to Dr. Rupert C. C. Perera of Lawrence Berkeley National Laboratory for his support of the spectroscopic measurements at ALS. This work is supported by a Grant-in-Aid from the Ministry of Education, Culture, Sports, Science and Technology of Japan under contract No. 17550090. Work also supported by the U.S. Department of Energy under Contract No. DE-AC02-05CH11231.

References

1. R. Kalish, *Diamond Relat. Mater*., **2001**, 10, 1749.

2. N. Fujimori, H. Nakahata and T. Imai*, Jpn. J. Appl. Phys*., **1990**, 29, 824.

3. H. Shiomi, Y. Nishibayashi, and N. Fujimori, *Jpn. J. Appl. Phys*., **1991**, 30, 1363.

4. J. Nakamura, K. Kabasawa, N. Yamada, Y. Einaga, D. Saito, H. Isshiki, S. Yugo, and R. C. C. Perera, *Phys. Rev*., **2004**, B 70, 245111.

5. J. Iihara, Y. Muramatsu, T. Takebe, A. Sawamura, A. Namba, T. Imai, J. D. Denlinger, and R. C. C. Perera, *Jpn. J. Appl. Phys*., **2005**, 44, 6612.

6. Y. Muramatsu, T. Takebe, A. Sawamura, J. Iihara, A. Namba, T. Imai, J. D. Denlinger, and R. C. C. Perera, *X-Ray Spectrometry*, **2007**, 36, 162.

7. E. A. Ekimov, V. A. Sidorov, E. D. Bauer, N. N. Mel'nik, N. J. Curro, J. D. Thompson, and S. M. Stishov, *Nature*, **2004**, 428, 542.

8. T. Yokoya, T. Nakamura, T. Matsushita, T. Muro, Y. Takano, M. Nagao, T. Takenouchi, H. Kawarada, and T. Oguchi*, Nature*, **2005**, 438, 647.

9. M. Hoesch, T. Fukuda, T. Takenouchi, JP. Sutter, S. Tsutsui, AQR. Baron, M. Nagao, Y. Takano, H. Kawarada, and J. Mizuki, *Science and Technology of Advanced Materials*, **2006**, 7, S31-S36, Sp. Iss., 1.

10. J. E.Holiday, *Adv. X-ray Anal*., **9**, 365 (1965).

11. D. W. Fischer and W. L. Baun, *J. Appl. Phys*., **37**, 768 (1966).

12. O. Aita and T. Sagawa, *J. Phys. Soc. Jpn*., **27**, 164 (1969).

13. V. A. Fomichev, T. M. Zimkina, and I. I. Lyakhovskaya, *Soviet Physics-Solid State*, **12**, 123 (1970).

14. M. Okusawa, Y. Iwasaki, K. Tsutsumi, M. Aono, and S. Kawai, *Jpn. J. Appl. Phys*., **17**, 161 (1978).

15. K. Tanaka, M. Yoshino, and K. Suzuki, *J. Phys. Soc. Jpn*., **51**, 382 (1982).

16. H. Kohzuki and M. Motoyama, *Adv. X-ray Chem. Anal. Jpn*., **23**, 43 (1992).

17. Y. Muramatsu, M. Oshima, T. Shoji, and H. Kato, *Rev. Sci. Instrum*., **63**, 5597 (1992).

18. E. Z. Kurmaev, A. V. Ezhov, S. N. Shamin, V. M. Cherkashenko, Yu. G. Andreev, and T.

Lundström, *J. Alloy and Compounds*, **248**, 86 (1997).

19. T. Kaneyoshi, H. Kohzuki, Y. Muramatsu, Y. Kowada, J. Kawai, and M. Motoyama, *X-Ray Spectrom*., **28**, 497 (1999).

20. R. H. Wentorf, *J. Phys. Chem*., **1971**, 75, 1833.

21. H. M. Strong and R. M. Chrenko, *J. Phys. Chem*., **1971**, 75, 1838.

22. H. Sumiya, N. Toda, and S. Satoh, *SEI (Sumitomo Electric Industries) Technical Review*, **2005**, 60, 10.

23. J. J. Jia, T. A. Callcott, J. Yurkas, A. W. Ellis, F. J. Himpsel, M. G. Samant, J. Stöhr, D. L. Ederer, J. A. Carlisle, E. A. Hudson, L. J. Terminello, D. K. Shuh, and R. C. C. Perera, *Rev. Sci. Instrum*., **1995**, 66, 1394.

24. Y. Ma, N. Wassdahl, P. Skytt, J. Guo, J. Nordgren, P. D. Johnson, J-E. Rubensson, T. Boske, W. Eberhardt, and S. D. Kevan, *Phys. Rev. Lett*., **1992**, 69, 2598.

25. Y. Muramatsu, Y. Tani, Y. Aoi, E. Kamijo, T. Kaneyoshi, M. Motoyama, J. J. Delaunay, T. Hayashi, M. M. Grush, T. A. Callcott, D. L. Ederer, C. Heske, J. H. Underwood, and R. C. C. Perera, *Jpn. J. Appl. Phys*., **1999**, 38, 5143.

26. H. Adachi, M. Tsukada, and C. Satoko, *J. Phys. Soc. Jpn*., **1978**, 45, 875.

27. C. Satoko, M. Tsukada, and H. Adachi, *J. Phys. Soc. Jpn*., **1978**, 45, 1333.

28. Y. Muramatsu, T. Kaneyoshi, E. M. Gullikson, and R. C. C. Perera, *Spectrochimica Acta*, **2003**, A59, 1951.

Figure Caption

Fig. 1 C*K* X-ray emission spectra of B-doped diamonds (CVD-B- and HPT-B-diamonds) and reference compounds of CVD-diamond, HPT-diamond, and HOPG.

Fig. 2 B*K* X-ray emission spectra of B-doped diamonds (CVD-B- and HPT-B-diamonds) and reference compounds of *h*-BN, *c*-BN, B_4C, and *a*-B.

Fig. 3 Upper panel shows the cluster model ($BC_{146}H_{148}$) for B-doped diamond where the terminating H atoms are not shown. Lower panel shows the calculated 2*p*- and 2*s*-DOS of the B and centered C atoms (denoted by asterisks in the cluster model) compared to the B*K* X-ray emission spectrum of CVD-B-diamond.

Fig. 4 Upper panel shows the cluster model ($B_{48}N_{48}H_{24}$) for *h*-BN where the terminating H atoms are not shown. Lower panel shows the calculated 2*p*- and 2*s*-DOS of the B and centered N atoms (denoted by asterisks in the cluster model) compared to the B*K* X-ray emission spectrum of HPT-B-diamond and *h*-BN.

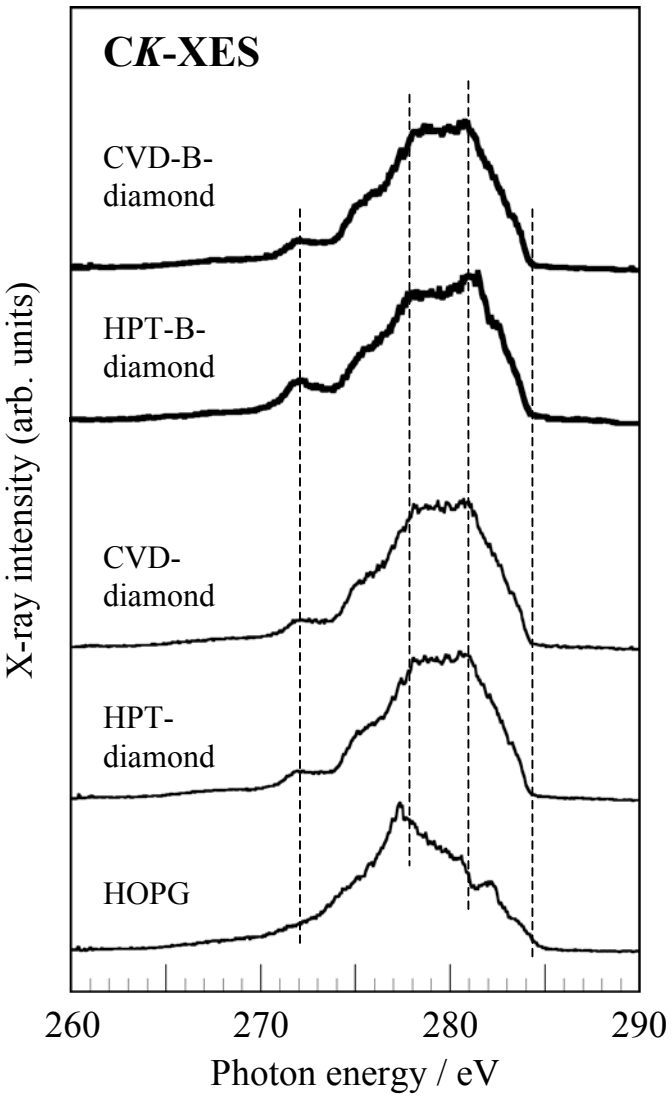

Figure 1 Y. Muramatsu et al.

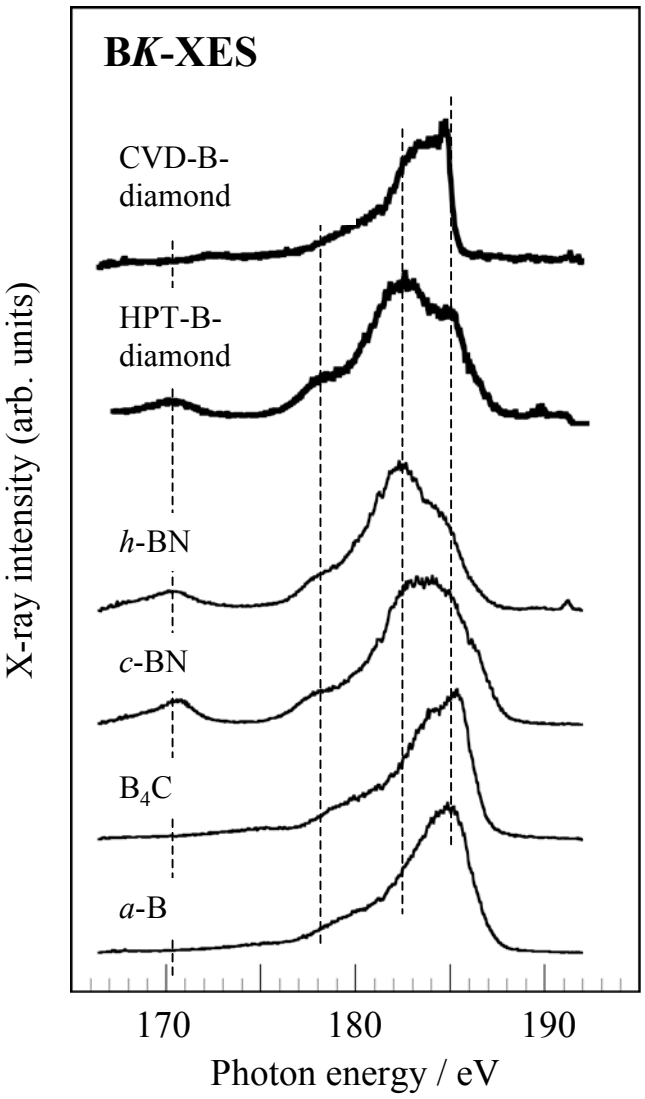

Figure 2 Y. Muramatsu et al.

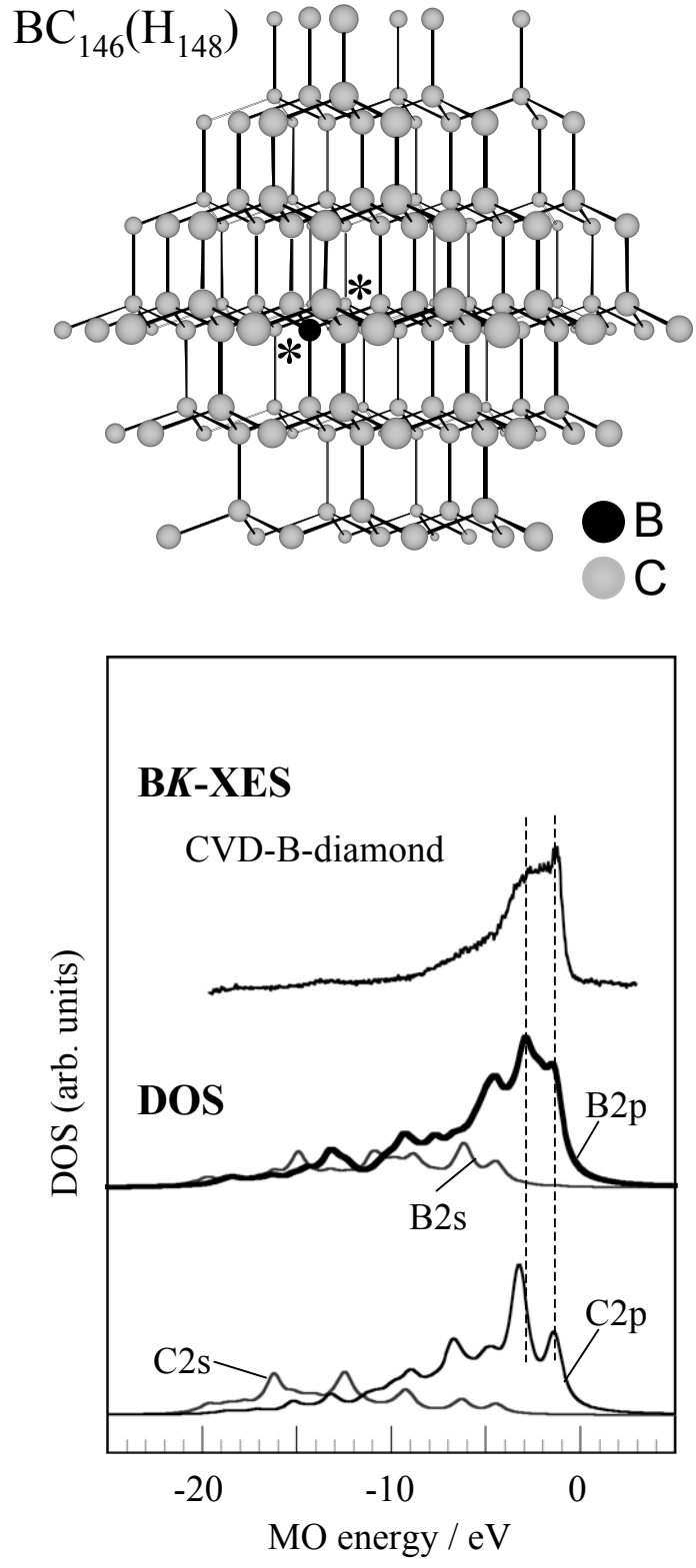

Figure 3 Y. Muramatsu et al.

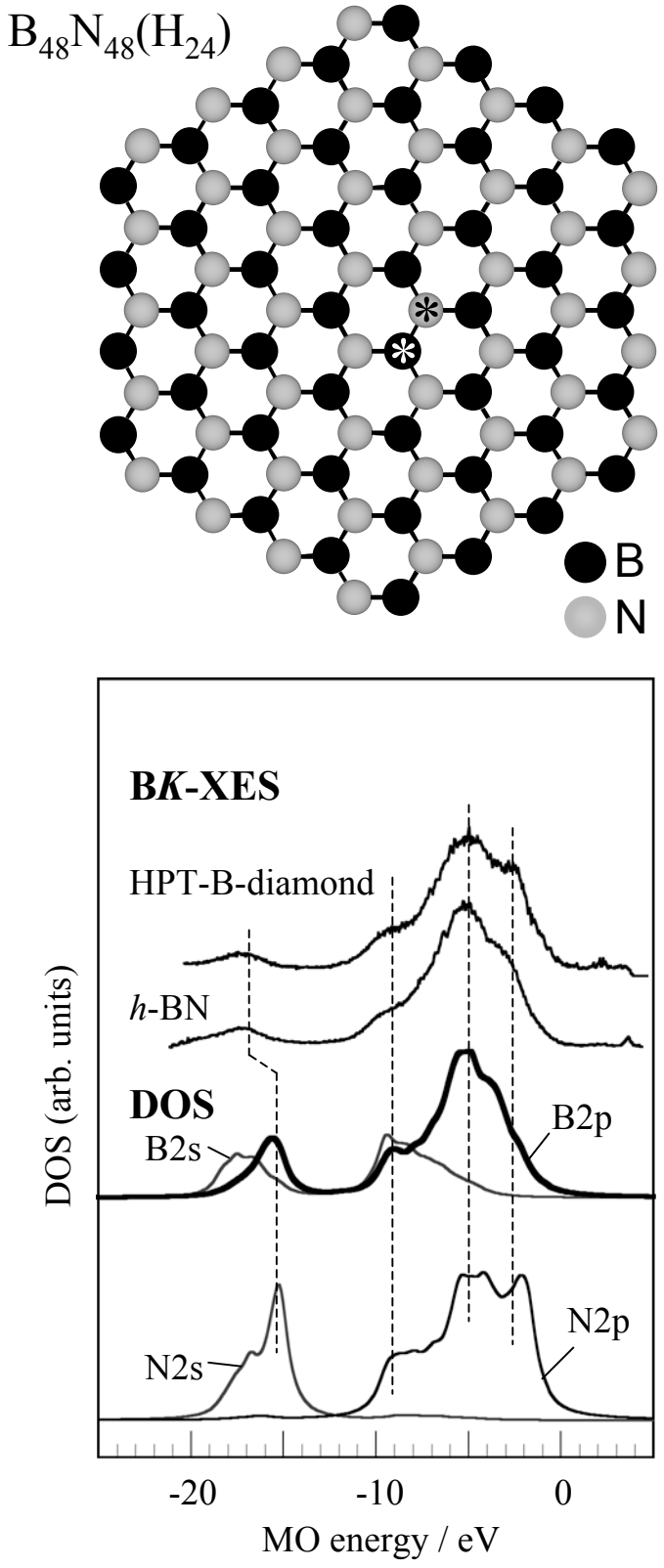

Figure 4 Y. Muramatsu et al.